Proc. Natl. Acad. Sci. USA
Vol. 87, pp. 1710–1714, March 1990
Biochemistry

Electron microscopy of small nuclear ribonucleoprotein (snRNP) particles U2 and U5: Evidence for a common structure-determining principle in the major U snRNP family

(splicing/snRNP structure/RNA–protein interaction/immunoelectron microscopy)

BERTHOLD KASTNER, MONTSERRAT BACH, AND REINHARD LÜHRMANN

Institut für Molekularbiologie und Tumorforschung der Philipps-Universität Marburg, Emil-Mannkopff-Strasse 2, D - 3550 Marburg, Federal Republic of Germany

Communicated by Phillip A. Sharp, December 14, 1989

ABSTRACT **We have studied by electron microscopy the structures of native small nuclear ribonucleoprotein (snRNP) particles U2 and U5 from HeLa cells. The structure of native U2 snRNP is characterized by a main body 8 nm in diameter with one additional domain about 4 nm long and 6 nm wide. Electron micrographs show that the 20S U5 snRNP, which contains at least seven U5-specific proteins in addition to the common proteins, has an elongated structure measuring 20–23 nm in length and 11–14 nm in width. Two main structural domains can be distinguished: a small head and a large elongated body about twice the size of the head. In addition to the head, the body of the 20S U5 snRNP possesses three short protuberances. The U2 and U5 core RNP particles—that is, of the snRNPs U2 and U5 without the snRNP-specific proteins, look much simpler and smaller under the electron microscope. They both are round in shape with a diameter of ≈8 nm. With respect to their size, appearance, and fine structure, the U2 and U5 snRNP cores not only closely resemble each other but also share these properties with the core domain of U1 snRNP. We propose that the characteristic shape of each of the major snRNP species U1, U2, U4/U6, and U5 is determined by (*i*) a core domain containing the proteins that are common to all members of this family, which has the same shape for each member, and (*ii*) peripheral structures, which for snRNPs U1, U2, and U5 arise from the specific proteins, that give each of these snRNP species its characteristic shape.**

Eukaryotic cells contain a group of small nuclear ribonucleoproteins (snRNPs), of which the principal members are snRNPs U1, U2, U4/U6, and U5 (1–4). These are involved in the splicing of mRNA and are part of spliceosomes (5–7). One function of the snRNPs appears to be the recognition of consensus sequence elements within pre-mRNA (8–12). Protein analysis of the snRNPs from metazoan cells (for review, see ref. 13) led to the identification of at least seven common proteins, denoted B′, B, D, D′, E, F, and G, that are present in every snRNP species. In addition, at least snRNPs U1, U2, and U5 are characterized by the presence of snRNP-specific proteins. Thus, U1 snRNP contains, in addition, the proteins 70k, A, and C; U2 contains the proteins A′ and B″; and U5 contains at least seven U5-specific proteins of molecular masses 40, 52, 100, 102, 116, and 200 kDa (a double band) (14). Owing to the large number of U5-specific proteins, these U5 snRNP particles sediment on sucrose gradients with an S value of 20 (14). Proteins specific to U4/U6 snRNP have not yet been identified in metazoan cells. A protein of molecular mass of ≈52 kDa, however, has recently been found to be bound specifically to U4 RNA in yeast (15, 16). It is likely that the snRNP-specific proteins are related to the individual functions of the respective snRNP particles in the splicing process (17–20).

The association of the same seven polypeptides (B′ to G) with various distinct small nuclear RNAs (snRNAs) suggests the possible existence of a common RNP core structure. The snRNAs also appear to provide for this because there is a structural motif common to the snRNAs U1, U2, U4, and U5, the so-called domain A (21), which consists of a single-stranded region $RA(U)_nGR$, with $n \geq 3$, flanked by double-stranded stems. The domain A is the only major piece of the snRNAs essential for assembling the common proteins into the snRNPs (22–24). In contrast, the specificity of interaction of the snRNP-characteristic proteins with their cognate RNP particles appears to be guided by direct protein–RNA interactions with snRNA-specific stem/loop structures. This fact has recently been demonstrated for some of the U1- and U2-specific proteins (25–30).

Knowing the three-dimensional structure of the U snRNPs will be important for understanding the way in which the various snRNPs interact with pre-mRNA sequences and with other factors in the spliceosome. As a step in this direction, we have started to investigate purified snRNPs at the ultrastructural level using electron microscopy. Thus, we were recently able to show that native U1 snRNPs consist of a main round-shaped body, 8 nm in diameter, with two characteristic protuberances 4–7 nm long and 3–4 nm wide (31). In the work described here, we have investigated by electron microscopy the structure of native snRNPs U2 and U5 and their respective cores—i.e., snRNP particles U2 and U5 that completely lack the U2- and U5-specific proteins. Our data indicate that the major U snRNPs share a core RNP domain (containing the common proteins) round in shape and ≈8 nm in diameter. The structure of this domain is very similar from one snRNP species to another. Our data suggest further that the characteristic dimensions and shape of each snRNP species is mainly determined by the number of snRNP-specific proteins and the manner in which they are attached to their cognate core RNP domains.

MATERIALS AND METHODS

Preparation of U snRNPs. The two types of U5 snRNPs—i.e., native 20S U5 snRNPs and core U5 snRNP particles, were isolated as described in detail elsewhere (14, 32). In summary, a mixture of snRNPs U1, U2, U5, and U4/U6 was first isolated by anti-2,2,7-trimethylguanosine (Me_3Guo) immunoaffinity chromatography (33) from HeLa nuclear extracts prepared by the method of Dignam *et al.* (34). The purified snRNPs U1–U6 were then resolved by fast protein liquid chromatography with a Mono Q ion-exchange column (Pharmacia) by elution with an increasing KCl gradient (50

The publication costs of this article were defrayed in part by page charge payment. This article must therefore be hereby marked "*advertisement*" in accordance with 18 U.S.C. §1734 solely to indicate this fact.

Abbreviations: snRNA, small nuclear RNA; snRNP, small nuclear ribonucleoprotein; Me_3Guo, 2,2,7-trimethylguanosine.

mM–1 M) in elution buffer (20 mM Tris·HCl, pH 7.5/1.5 mM $MgCl_2$/0.5 mM phenylmethylsulfonyl fluoride/0.5 mM dithiothreitol). The identity of the RNA and protein constituents of the fractions was then determined by electrophoresis, as described by Bringmann *et al.* (33). The 20S U5 snRNPs—i.e., those U5 snRNPs containing the full complement of U5-specific proteins, were eluted together with a small amount of U1 snRNPs at a chloride concentration of ≈340 mM. The 10S U5 snRNP—i.e., the core U5 snRNP lacking the U5-specific proteins, eluted at a chloride concentration of ≈450 mM together with a fraction of U2 snRNPs and residual amounts of U1 snRNPs. U2 snRNPs lacking proteins A′ and B″ eluted at a chloride concentration of ≈550 mM. Essentially pure 10S U5 snRNPs were obtained by Mono Q chromatography by using a less steep KCl salt gradient for the elution. Pure 20S U5 snRNPs were obtained by subjecting the U5 and U1 snRNP fractions obtained from the Mono Q column to centrifugation in a 5–20% (vol/vol) glycerol gradient in elution buffer containing 150 mM KCl. The gradients were centrifuged in a Beckman SW60 Ti rotor at 84,000 × *g* for 20 hr.

Native U2 snRNPs were isolated from splicing extracts that had already been depleted of the majority of their endogenous U1 snRNPs by one passage over an anti-Me_3Guo column under conditions allowing preferential adsorption of U1 snRNPs to the anti-Me_3Guo antibodies (32). After a second anti-Me_3Guo-affinity chromatography, the respective Me_3Guo eluate containing a mixture of snRNPs highly enriched in U2 and U4/U6 snRNPs was subjected to Mono Q chromatography as described above. Native U2 snRNPs eluted at a chloride concentration of ≈480 mM.

Immunocomplex Formation Between 20S U5 snRNPs and Anti-Me_3Guo Antibodies. 20S U5 snRNPs (15 μg) were incubated for 60 min at 0°C with 2 μg of monoclonal anti-Me_3Guo IgG H-20·(35) in 25 μl of buffer A (20 mM Hepes·KOH, pH 7.9/150 mM KCl/1.5 mM $MgCl_2$). After dilution with a further 75 μl of buffer A, the mixture was loaded onto a 10–30% (vol/vol) glycerol gradient (1 ml) in buffer A and centrifuged for 4.5 hr at 50,000 rpm in a TLS-55 rotor (Beckman). The gradient was fractionated in 60-μl portions from the bottom.

Electron Microscopy. Glycerol gradient fractions containing purified 20S U5 snRNP particles or 20S (U5 snRNP·H-20 IgG) immunocomplexes, or Mono Q fractions containing the U2 snRNPs or the core RNP particles of snRNPs U2 and U5 were used directly for the preparation of samples for electron microscopy. Negative staining with 2.5% uranyl formate was carried out by the double carbon film method as described (31). The preparations were examined under a Zeiss EM 109 electron microscope with an acceleration voltage of 80 kV, and electron micrographs were taken with magnifications between 85,000 and 140,000.

RESULTS

Preparation of Native snRNPs U2 and U5 and of Their Core RNP Particles. The U5 snRNP particles used for electron microscopy were isolated from HeLa nuclear splicing extracts by the successive application of anti-Me_3Guo immunoaffinity chromatography, Mono Q ion-exchange chromatography, and centrifugation in glycerol gradients. Two types of U5 snRNP particles can be obtained in this way, with respective sedimentation values of 20S and 10S. Their protein and RNA compositions are shown in Fig. 1. In addition to the common proteins B′, B, D, D′, E, F, and G, the 20S U5 snRNP particle contains a number of U5-specific proteins characterized by molecular masses of 40, 52, 100, 102, 116, and 200 kDa (mostly a double band) (Fig. 1*A*, lane I). The isolated 20S U5 snRNPs are functionally active in a splicing system *in vitro* (36). The 10S U5 snRNP particle contains the common proteins only (Fig. 1*A*, lane II), and this particle is considered to represent the core U5 snRNP structure that has lost the U5-specific proteins during the various isolation steps.

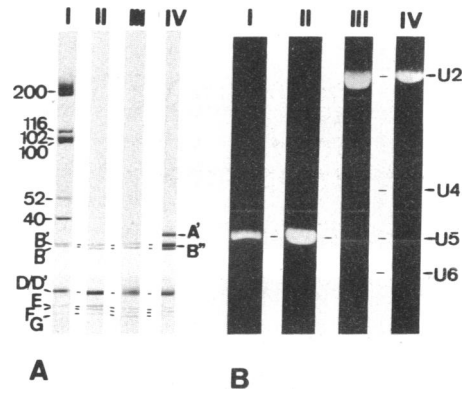

FIG. 1. Polypeptide and RNA composition of the purified U5 snRNPs and their core particles. After extraction with phenol/chloroform and electrophoresis on a 4–20% SDS/polyacrylamide gradient gel, the proteins were stained with Coomassie blue (*A*). The RNA of the snRNPs was separated by electrophoresis on a urea/polyacrylamide gel and stained with ethidium bromide (*B*). Lanes: I, 20S U5 snRNPs; II, core U5 snRNPs; III, core U2 snRNPs; and IV, U2 snRNPs. Numbers at left represent kDa.

Using the same protocol as described for U5 snRNPs but omitting the centrifugation step in glycerol gradients, we also obtained two types of U2 snRNP. These were U2 snRNPs containing the U2-specific proteins A′ and B″ in addition to the common proteins (native U2 snRNPs) and core U2 snRNPs that lack the U2-specific proteins but have retained all the common proteins (Fig. 1*A*, lanes III and IV).

Electron Microscopy of 20S U5 snRNPs. The 20S U5 snRNP particles isolated from the glycerol gradient (the final purification step) were adsorbed onto carbon films and, after negative staining with uranyl formate, used directly for electron microscopy. Fig. 2*A* shows a representative electron micrograph. In general, the particles have an elongated form. Owing to accumulation of stain, a segmentation line can be seen that divides the U5 snRNP particle into an upper third and a lower two-thirds, denoted head and body, respectively. One or two protuberances extend from the lower pole of the body, while another may be seen on the right-hand side of the body close to the dividing line between body and head.

Detailed examination of ≈500 views of 20S U5 snRNP particles led to the recognition of six representative forms that accounted for >60% of the particles. Three typical views of each of the six representative forms are shown in Fig. 2*B*. All particles are displayed with the head pointing upwards. The various U5 snRNP forms differ in their body structure, in particular in the number and appearance of the short protuberances extending from the body. The first three rows (Fig. 2*B*) display frequently observed forms (each form is present in >40% of the particles), while the last three show rare, but typical forms.

The top row displays a U5 snRNP form with two protuberances at the lower pole of the body, which point away from each other. In most cases, the left protuberance appears to be more pronounced than the lower right one. A further characteristic feature of this form is the presence of a third protuberance on the upper right of the body, extending from just below the dividing line between head and body. The outline of this form is shown in Fig. 2*C* to illustrate the characteristic features of the 20S U5 snRNP particle.

Typical of the form shown in row II (Fig. 2*B*) is that only one protuberance, with a paler tip, can be seen attached to the very bottom of the body. The absence of the upper right protuberance gives this form a rather extended rod-like shape. In the form shown in row III of Fig. 2*B*, the major lower protuberance, as described above, now points to the right, and a less pronounced protuberance can be seen on the

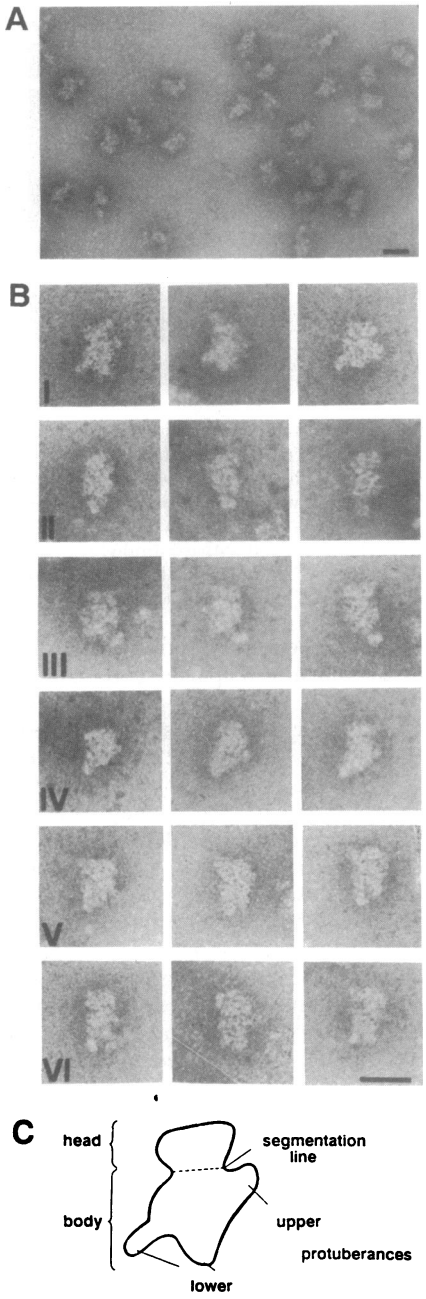

FIG. 2. 20S U5 snRNPs negatively stained with uranyl formate. (*A*) Representative general view. (*B*) Six representative forms of 20S U5 snRNP particles. Three typical views for each representative form are shown in each row. The micrographs are oriented such that the heads of the U5 snRNPs point upwards. (Bar = 20 nm.) (*C*) Illustrative sketch of the 20S U5 snRNP with the nomenclature of the characteristic features, as used in text.

left-hand side of the body. An approximate mirror image of this form is the rarer form seen in row IV. The most characteristic feature of the form shown in row V of Fig. 2 is a short extension that protrudes from the left-hand side of the head, giving this form an asymmetric shape. In contrast, the form in row VI is a more symmetric one; this is due mainly to the similar appearance of the two lower protuberances.

The sizes of the various 20S U5 snRNP images shown in Fig. 2 are, in general, similar—the head and body being 20–23 nm long and 11–14 nm wide, depending on the appearances of the protuberances on the body. Forms in which particular protuberances are not recognizable could correspond to particles that have lost one or more of the U5-specific proteins (see below). An alternative and more likely explanation for the observation of different forms is their different orientation on the carrier film, as previously discussed in the case of U1 snRNPs (31).

Electron Microscopy of Core U5 snRNP Particles. Next, we investigated the structure of the 10S U5 snRNPs lacking the U5-specific proteins while still containing the set of common proteins B′, B, D, D′, E, F, and G (Fig. 1*A*, lane II). A general field of negatively stained U5 snRNP cores is shown in Fig. 3*A*. In contrast to the elongated and indented shape of the 20S U5 snRNPs described above, the core U5 snRNP particles are, more or less, round in shape. Furthermore, the U5 cores are much smaller than the 20S U5 snRNPs, with a diameter of ≈8 nm. On close inspection of individual views, further structural details may be recognized; these are due to regions of high stain density within the round core structure (Fig. 3*B*). Quite often, forms are seen with a line of stain that roughly bisects the core (rows I and II). In rare cases, a short extension 3–4 nm long, may be seen protruding from the round core structure (row II). Sometimes two lines of dark stain produce a wedge-shaped structure within the U5 snRNP core (row III). Core U5 snRNPs marked by a lighter or darker central dot (rows IV and V, respectively) also occur with the same frequency as the particles described above.

Localization of the 5′ End of U5 RNA at the Surface of 20S U5 snRNPs. Owing to the large difference in size and appearance of the 20S and 10S U5 snRNPs, the U5 snRNP core could not be assigned with any certainty to a particular structural feature of the 20S U5 snRNP particle, such as the head or a part of the body (compare Figs. 2 and 3). We therefore decided to use immunoelectron microscopy to localize the 5′ end of the U5 RNA at the surface of the 20S U5 snRNP particle, reasoning that with this information we could roughly locate the core domain within the elongated 20S U5 snRNP structure.

The immunoelectron microscopic localization of the 5′ end at the surface of 20S U5 snRNPs was carried out with monoclonal anti-Me_3Guo antibody H-20, essentially as described previously for U1 snRNPs (31). Immunocomplexes in which one IgG molecule was bound to one 20S U5 snRNP particle predominated, whereas U5–IgG–U5 complexes were rare (<5%). Reaction of monoclonal antibody H-20 with 20S U5 snRNPs was specific insofar as preincubation of the antibody molecules with excess cross-reactive nucleoside 7-methylguanosine completely abolished immunocomplex formation (data not shown).

More than 200 micrographs (U5 snRNP·H-20 IgG) immunocomplexes were investigated. It is important to note that the various principal forms of free 20S U5 snRNPs (as defined in Fig. 2) could also be recognized when the U5 snRNP particles were attached to the anti-Me_3Guo antibody. This

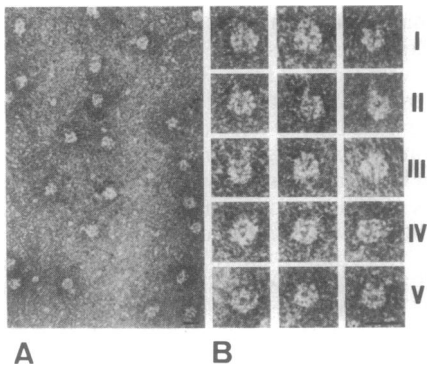

FIG. 3. Core U5 snRNPs negatively stained with uranyl formate. (*A*) General field. (*B*) Gallery of typical views. Each row shows three views of core U5 snRNPs that share fine structural details as described in text. (Bar = 10 nm.)

allowed the Me_3Guo cap to be located with relative accuracy. Fig. 4*A* shows representative examples of these immunocomplexes, grouped in such a way that each row displays U5 snRNP–IgG complexes with similar U5 snRNP forms. Row VI of Fig. 4*A* shows examples of the rare cases in which one IgG molecule is attached simultaneously to two U5 snRNPs. It is clear from these electron micrographs that the 5′-terminal Me_3Guo cap of U5 RNA is located at the bottom of the body of the 20S U5 snRNP, close to the region where the bases of the two lower protuberances of the body approach each other. When the same experiment was carried out with core U5 snRNPs, the Fab arms of the anti-Me_3Guo molecules were always found attached close to the surface of the core structure (data not shown). This agrees well with the secondary structure model of U5 RNA, where the 5′ end of U5 RNA is positioned close to the domain A—i.e., the binding site of the core RNP proteins.

Therefore, in the 20S U5 snRNP structure the core domain is most probably located at the bottom of the body (see Fig. 4*B* for an interpretative drawing).

Electron Microscopy of U2 snRNPs. Fig. 5*A* shows a general view of native U2 snRNPs that contain the U2-specific proteins A′ and B″ in addition to the common proteins. Most images exhibit slightly elongated forms, and two structural domains can be distinguished: a main body, round in shape and ≈8 nm in diameter, and a smaller domain, 6 nm wide and

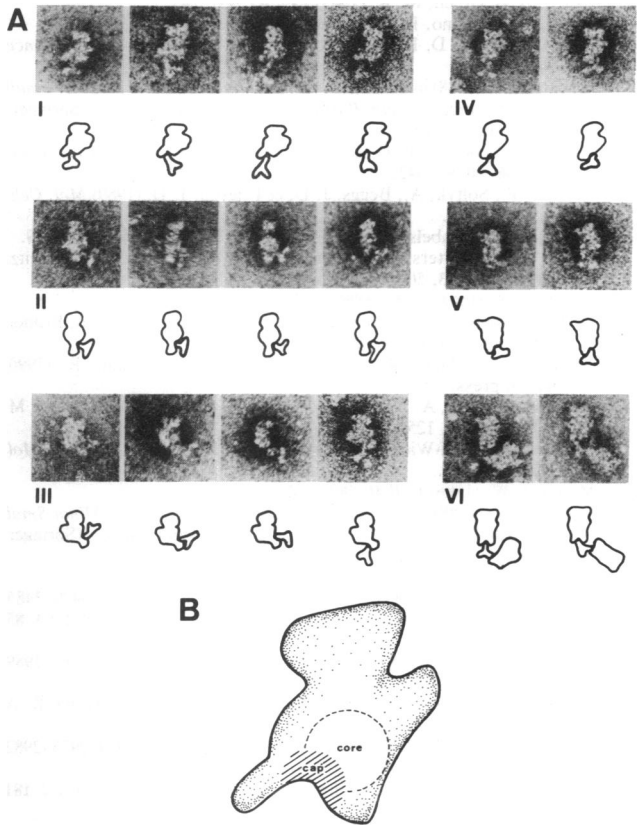

FIG. 4. Anti-Me_3Guo antibody binding to 20S U5 snRNPs. (*A*) Selected electron micrographs of negatively stained anti-Me_3Guo (U5 snRNP·H20 IgG) immunocomplexes. In the immunocomplexes the same representative forms of 20S U5 snRNPs as defined in Fig. 3 could be recognized, which are illustrated by four views (rows I–III) or two views (rows IV–VI) each. (*B*) Interpretative drawing of the U5 snRNP showing the location of the U5 snRNP 5′-terminal cap as determined by immunoelectron microscopy (hatched area). A possible position of the round-shaped core domain (dotted line) close to the cap site is shown as well. Its positioning on the lower right-hand side of the body is arbitrarily chosen; it may equally well be located on the lower left-hand side of the body.

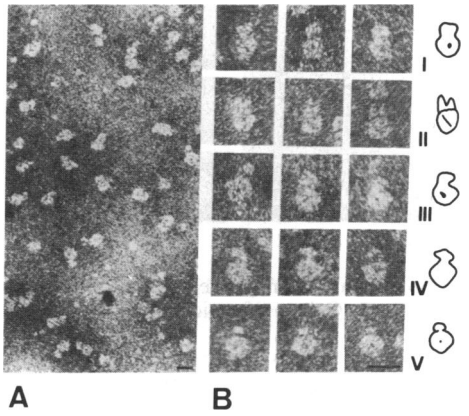

FIG. 5. U2 snRNPs negatively stained with uranyl formate. (*A*) General field. (*B*) Gallery of typical views. Each row shows three areas that share fine structural details as described in text and illustrated in the interpretative drawing at right. The micrographs are oriented such that the head of the U2 snRNP points upwards. (Bar = 10 nm.)

≈4 nm long, attached to the body, which we shall here call the head domain.

Typical U2 snRNP images are shown in Fig. 5*B*. The images are oriented so that the head points upwards. The images shown in rows I–V differ especially in the appearance of the head domain. Most images appear symmetric, as shown in row I. In rare cases, a slight indentation, due to accumulation of stain, can be seen in the middle of the head domain (row II). Other images show the head domain pointing either to the right (row III) or to the left (row IV). In about a quarter of the U2 snRNP images, only a rudimentary head domain can be seen attached to the body (row V).

The main body of U2 snRNPs shows striking morphological similarities with the core domain of U5 snRNPs. This is not only true of the dimensions of the body; it also applies to the fine structural details seen in the U5 RNP core, as discussed above (compare Figs. 3 and 5*B*). It may thus be suggested that the main body of the U2 snRNPs represents the core RNP domain, whereas the additional head domain should represent the U2-specific proteins A′ and B″.

Electron Microscopy of U2 Core snRNP Particles. The above hypothesis received support from the examination of U2 snRNP cores lacking the U2-specific proteins under the electron microscope. The U2 snRNP cores are round, ≈8 nm in diameter, and lack the head-like structure typical of U2 snRNPs containing proteins A′ and B″ (Fig. 6*A*). At higher magnification, further structural details can be seen within the round core structure. These are caused by regions of high stain density, such as dots or lines of stain roughly bisecting the core (Fig. 6*B*).

DISCUSSION

In this work we have applied the technique of electron microscopy to study the structure of isolated snRNP particles U2 and U5 from HeLa cells. The native U5 snRNP has an elongated and highly indented shape 20–23 nm long and 11–14 nm wide. It is the largest of all U snRNPs investigated up to now, which correlates well with its high sedimentation coefficient of 20S. The structure of the native U2 snRNP particle can easily be distinguished from U5 snRNPs. U2 snRNPs are smaller, measuring ≈12 nm in length and between 6 and 8 nm in width. Two structural domains may be distinguished: a round-shaped main body, of ≈8-nm diameter, to which one smaller domain ≈6 nm wide and 4 nm long is attached.

The typical distinguishing structural features of the native snRNPs U2 and U5 are completely lost when only their core RNP structures are examined. This is the case for the incomplete snRNPs U2 and U5 that consist only of the

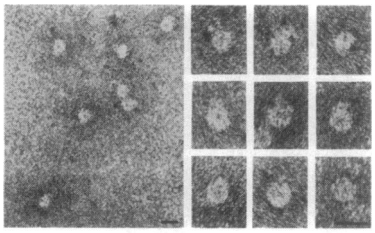

FIG. 6. Core U2 snRNPs negatively stained with uranyl formate. (*A*) General field. (*B*) Gallery of typical views. (Bar = 10 nm.)

respective RNA molecules and the common proteins B′ to G. The U2 and U5 cores both consist of a round body ≈8 nm in diameter and even share certain structural details, such as a central dark dot or a line of stain roughly bisecting the body. It is striking that a round body ≈8 nm in diameter, exhibiting the same internal structural details as discussed above for the U2 and U5 RNP cores, was also recently identified as one main structural feature of native U1 snRNPs (31). In contrast, the shape of native U1 snRNPs is characterized by two elongated protuberances attached to the round main body, which allows easy distinction between native snRNP particles of the types U1, U2, and U5. The observed structural similarities between the main body of U1 snRNP and the U2 and U5 core RNP particles suggest that the U1 snRNP body might also represent its core RNP domain containing the common proteins. Finally, purified snRNPs U4/U6 also contain a round-shaped body 8 nm in diameter as one main structural feature (unpublished work).

Our data suggest a common structure-determining principle for the major U snRNPs. On the one hand, the snRNPs U1, U2, U5, and U4/U6 share a morphologically very similar round-shaped core RNP domain that consists of the common proteins B′, B, D, D′, E, F, and G and the domain A of the respective snRNA molecules. On the other hand, the characteristic and distinguishing shape of each snRNP species appears to be due mainly to the number of the respective snRNP-specific proteins and the manner in which these are attached to the structurally very similar core RNP domains.

Given the likely possibility that the additional structural domains (protuberances or head structures extending from the main body of the U2 or U5 RNP cores) represent snRNP-specific proteins, some conclusions may be drawn concerning the binding sites of the specific proteins on their respective RNP core domains. Thus, the fact that only one additional domain can be seen attached to the round core RNP body in native U2 snRNPs suggests that proteins A′ and B″ are bound together to a topologically restricted area on the U2 RNP particle and may even interact with each other in the native U2 snRNP. Other studies have suggested that the B″ protein may interact with stem loop III of U2 RNA (25, 30), whereas no direct interaction of the A′ protein with U2 RNA has yet been reported. Unlike the situation in U2 snRNPs, the attachment of several protuberances including the head and body of the 20S U5 snRNP suggests that several of the U5-specific proteins should have independent binding sites at the U5 snRNP core.

How does the complex structure of the 20S U5 snRNP, as observed under the electron microscope, relate to the function of this particle in splicing? It has recently been demonstrated that U5 snRNP is essential for the second step of splicing and is further needed for efficient completion of the first splicing reaction (36, 37). In the spliceosome U5 snRNP interacts with other snRNPs such as the U4/U6 snRNP and possibly also with snRNPs U1 and U2 (38–41). Furthermore, the U5 snRNP appears to recognize the 3′ end of the intron (12, 18, 19) and remains associated with the excised intron lariat. Thus, U5 snRNP may be considered as a scaffold on which several other components assemble in the spliceosome. The large size of U5 snRNP, with the multiple protein-containing domain extending from the RNP particle, could provide the structural basis for specific interactions of U5 snRNP in the spliceosome.

We are grateful to Vicki Sumpter for critical reading and Verena Buckow for typing the manuscript. We thank Irene Öchsner-Welpelo and Dorit Zeuske for excellent technical assistance. This work was supported by the Deutsche Forschungsgemeinschaft (SFB 272/A3). M.B. was supported, in part, by a fellowship from the Alexander von Humboldt-Stiftung.

1. Lerner, M. R. & Steitz, J. A. (1979) *Proc. Natl. Acad. Sci. USA* **76,** 5495–5499.
2. Reddy, R. & Busch, H. (1983) *Prog. Nucleic Acid Res. Mol. Biol.* **30,** 127–162.
3. Brunel, C., Sri-Widada, J. & Jeanteur, P. (1985) *Prog. Mol. Subcell. Biol.* **9,** 1–52.
4. Reddy, R. & Busch, H. (1988) in *Structure and Function of Major and Minor Small Nuclear Ribonucleoprotein Particles*, ed. Birnstiel, M. L. (Springer, New York), pp. 1–37.
5. Sharp, P. A. (1987) *Science* **235,** 766–771.
6. Maniatis, T. & Reed, R. (1987) *Nature (London)* **325,** 673–678.
7. Steitz, J. A., Black, D. L., Gerke, V., Parker, K. A., Krämer, A., Frendewey, D. & Keller, W. (1988) in *Structure and Function of Major and Minor Small Nuclear Ribonucleoprotein Particles*, ed. Birnstiel, M. L. (Springer, New York), pp. 115–154.
8. Black, D. L., Chabot, B. & Steitz, J. A. (1985) *Cell* **42,** 737–750.
9. Zhuang, Y. & Weiner, A. W. (1986) *Cell* **46,** 827–835.
10. Ruskin, B. & Green, M. R. (1985) *Cell* **43,** 131–142.
11. Parker, R., Siliciano, P. G. & Guthrie, C. (1987) *Cell* **49,** 229–239.
12. Chabot, B., Black, D. L., LeMaster, D. M. & Steitz, J. A. (1985) *Science* **230,** 1344–1349.
13. Lührmann, R. (1988) in *Structure and Function of Major and Minor Small Nuclear Ribonucleoprotein Particles*, ed. Birnstiel, M. L. (Springer, New York), pp. 71–99.
14. Bach, M., Winkelmann, G. & Lührmann, R. (1989) *Proc. Natl. Acad. Sci. USA* **86,** 6038–6042.
15. Bjorn, S. P., Soltyk, A., Beggs, J. D. & Friesen, J. D. (1989) *Mol. Cell. Biol.* **9,** 3698–3709.
16. Bauroques, J. & Abelson, J. N. (1989) *Mol. Cell. Biol.* **9,** 3710–3719.
17. Mount, S. M., Pettersson, I., Hinterberger, M., Karmas, A. & Steitz, J. A. (1983) *Cell* **33,** 509–518.
18. Gerke, V. & Steitz, J. A. (1986) *Cell* **47,** 973–984.
19. Tazi, J., Alibert, C., Temsamani, J., Reveillaud, I., Cathala, G., Brunel, C. & Jeanteur, P. (1986) *Cell* **47,** 755–766.
20. Heinrichs, V., Bach, M., Winkelmann, G. & Lührmann, R. (1990) *Science*, in press.
21. Branlant, C., Krol, A., Ebel, J. P., Lazar, E., Haendler, B. & Jacob, M. (1982) *EMBO J.* **1,** 1259–1265.
22. Liautard, J. P., Sri-Widada, J., Brunel, C. & Jeanteur, P. (1982) *J. Mol. Biol.* **162,** 623–643.
23. Mattaj, I. W. (1986) *Cell* **46,** 905–911.
24. Mattaj, I. W. (1988) in *Structure and Function of Major and Minor Small Nuclear Ribonucleoprotein Particles*, ed. Birnstiel, M. L. (Springer, New York), pp. 100–114.
25. Mattaj, I. W. & DeRobertis, E. M. (1985) *Cell* **40,** 111–118.
26. Hamm, J., Kazmaier, M. & Mattaj, I. W. (1987) *EMBO J.* **6,** 3479–3485.
27. Patton, J. R. & Pederson, T. (1988) *Proc. Natl. Acad. Sci. USA* **85,** 747–751.
28. Patton, J. R., Habets, W., van Venrooij, W. J. & Pederson, Th. (1989) *Mol. Cell. Biol.* **9,** 3360–3368.
29. Surowy, C. S., van Santen, V. L., Scheib-Wixted, S. M. & Spritz, R. A. (1989) *Mol. Cell. Biol.* **9,** 4179–4186.
30. Lutz-Freyermuth, C. & Keene, J. D. (1989) *Mol. Cell. Biol.* **9,** 2975–2982.
31. Kastner, B. & Lührmann, R. (1989) *EMBO J.* **8,** 227–286.
32. Bach, M., Bringmann, P. & Lührmann, R. (1990) *Methods Enzymol.* **181,** 232–257.
33. Bringmann, P., Rinke, J., Appel, B., Reuter, R. & Lührmann, R. (1983) *EMBO J.* **2,** 1129–1135.
34. Dignam, J. D., Lebovitz, R. M. & Roeder, R. D. (1983) *Nucleid Acids Res.* **11,** 1475–1489.
35. Bochnig, P., Reuter, R., Bringmann, P. & Lührmann, R. (1987) *Eur. J. Biochem.* **168,** 461–467.
36. Winkelmann, G., Bach, M. & Lührmann, R. (1989) *EMBO J.* **8,** 3105–3112.
37. Patterson, B. & Guthrie, C. (1987) *Cell* **49,** 613–624.
38. Grabowski, P. J., Seiler, S. R. & Sharp, P. A. (1985) *Cell* **42,** 345–353.
39. Konarska, M. M. & Sharp, P. A. (1987) *Cell* **49,** 763–774.
40. Lossky, M., Anderson, G. J., Jackson, S. P. & Beggs, J. (1987) *Cell* **51,** 1019–1026.
41. Lamond, A. I., Konarska, M. M., Grabowski, P. J. & Sharp, P. A. (1988) *Proc. Natl. Acad. Sci. USA* **85,** 411–415.